

Distributed Aerial Processing for IoT-Based Edge UAV Swarms in Smart Farming

Anandarup Mukherjee¹, Sudip Misra

Department of Computer Science and Engineering, Indian Institute of Technology Kharagpur, India, 721302

Anumandala Sukrutha

Department of Electrical Engineering, Indian Institute of Technology Hyderabad, Telangana State, India, 502285

Narendra Singh Raghuwanshi

Department of Agriculture & Food Engineering, Indian Institute of Technology Kharagpur, India, 721302

Abstract

This work addresses the challenges of a decentralized and heterogeneous Unmanned Aerial Vehicle (UAV) swarm deployment – some fitted with multimedia sensors, while others armed with scalar sensors – in resource-constrained and challenging environments, typically associated with farming. Subsequently, we also address the resulting problem of sensing and processing resource-intensive data aerially within the Edge swarm in the fastest and most efficient manner possible. The heterogeneous nature of the Edge swarm results in under-utilization of the available computation resources due to unequal data generation within its members. To address this, we propose a Nash bargaining-based weighted intra-Edge processing offload scheme to mitigate the problem of heavy processing in some of the swarm members. We do this by distributing the data to be processed to all the swarm members. Real-life hardware tuned simulation of a large UAV swarm shows that by increasing the number of UAVs in the swarm, our scheme achieves better scalability and reduced processing delays for intensive processing tasks. Additionally, in comparison to regular star and mesh topologies, our scheme achieves an increase in collective available network processing speeds by 100% for only 25% of the number of UAVs in a star topology.

Keywords: UAV swarm, collaborative processing, aerial mesh network, heterogeneous swarm, Edge computing, smart farming.

1. Introduction

Internet of Things (IoT) is in the process of revolutionizing agriculture through smart farming. The involvement of IoT in farming applications such as precision agriculture, livestock management, inventory management, and others has increased the productivity, yield, and raised economic benefits to farmers through connected sensors, actuators, and networked systems. UAVs – one of the prime examples of such networked system – has become quite popular in smart farming applications,

Email address: anandarupmukherjee@gmail.com (Anandarup Mukherjee)

7 with applications ranging from monitoring of crop health, farmland demarcation and mapping, to
 8 spraying fertilizers and pesticides periodically and autonomously.

9 Networked UAVs [1] are in extensive use for a range of solutions with far-reaching implications
 10 in the domains of agriculture, remote sensing, surveillance, security, law enforcement, disaster man-
 11 agement [2], and others. Most of these domains deal with UAV-based multimedia data for various
 12 tasks such as target tracking, information gathering, and path planning [3]. The real-time processing
 13 of multimedia data in constrained environments is an inherent problem, which is often encountered
 14 by UAVs in precision agriculture tasks. The data gathered from the farmlands, as well as the ones
 15 generated within the UAVs for its flight controls and navigation, are quite massive. Commonly, the
 16 data is stored within the UAVs and retrieved later for processing and analysis. However, this results
 17 in a loss of real-timeliness, which also prevents the implementation of complete UAV automation
 18 for agricultural practices. The biggest challenge faced during the implementation of a real-time
 19 UAV-based sensing solution by making use of multimedia data is the low computational power and
 20 limited energy resources of these UAVs.

21 Various solutions are proposed to address the problems of low computation capability of such
 22 UAVs. Solutions such as cloud-based data processing offloading from single UAVs [4], processing
 23 offloading from a UAV to a ground server [5], and others [6] offer limited respite from the challenges
 24 at hand as these are heavily dependent on network connectivity, bandwidth, and quality of service
 25 for reliable and timely operation. Additionally, the areas of implementation of such multi-UAV net-
 26 worked solutions may not always promise the availability of network connectivity, network quality, or
 27 bandwidth, especially in applications involving operations in remote and infrastructure-constrained
 28 applications such as agriculture and disaster management.

29 UAV deployment strategies for farming applications such as crop monitoring, field surveys, and
 30 others range from a single standalone powerful UAV to swarms of smaller, less powerful UAVs working
 31 in tandem. However, the use of multiple smaller UAVs has proved to be more efficient than a single
 32 large one regarding scalability, survivability, speed, cost, and bandwidth requirements [5]. Star and
 33 mesh network configurations are the commonly used topologies used for multi-UAV networks. In
 34 a star topology formation, each UAV connects to a central UAV, which, however, restricts direct
 35 communication between the UAVs in the network. Whereas, multi-UAV networks following a mesh
 36 topology allow direct or hop-based intra-member UAV to UAV communication within the network,
 37 however, at the cost of increased network load and traffic [5].

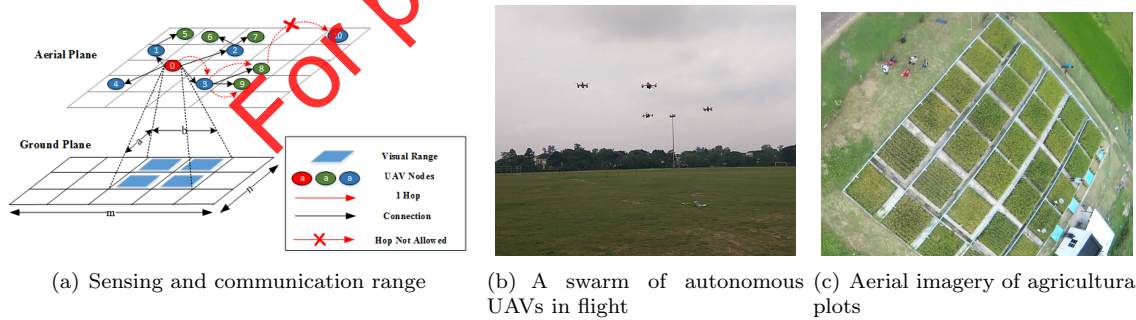


Figure 1: Edge UAV swarm-based operations and its possible applications in smart farming.

38 In this work, we propose a two-pronged approach to address the need for time-critical observation
 39 and tracking of ground-based tasks such as crop health and stress monitoring, farmland mapping
 40 (refer to Fig. 1(c)), and others by a heterogeneous collaborative sensing approach, which uses both

41 multimedia and scalar sensor armed UAVs in the swarm (refer to Fig. 1(b)). We additionally devise
 42 a scheme to mitigate the processing overheads of each swarm member, essentially an Edge computing
 43 platform, using distributed collaborative processing within the Edge UAV swarm itself.

44 **Assumption 1.** *A single Edge UAV in the swarm is equipped with a camera, whereas the other*
 45 *swarm members are equipped only with scalar sensors.*

46 **Assumption 2.** *A UAV with a camera sensor (which can be an RGB, thermal, or a multispectral*
 47 *camera) has a sensing range of $a \times b$, which is much larger than that of a UAV with a scalar sensor*
 48 *with a sensing range of only $a/2 \times b/2$. We consider the scalar sensing range as a single grid location*
 49 *in this work. \mathcal{L}_i represents the i^{th} grid location covered by a UAV.*

50 Fig. 1(a) shows the sensing and communication range of multiple UAVs in the swarm. In the
 51 aerial plane, the central UAV – node 0 – consists of a camera sensor, whereas the other UAVs (nodes
 52 1-10) consist of scalar sensors only. A much broader search area can be covered by either scaling-up
 53 the Edge-based swarm or by using multiple such Edge-based swarms. Additionally, we consider that
 54 a UAV with the camera can visually search 4 grids at the same time the other scalar sensor armed
 55 UAVs take to search a single grid each. For rs_i denoting the sensing range of the i^{th} UAV in the
 56 swarm at any instant of time, the camera-armed UAV's sensing range $rs_0 = a \times b$, whereas the scalar
 57 sensor fitted UAV's sensing range $rs_{1-7} = a/2 \times b/2$. The communication range between a source
 58 (S) and destination (D) UAV node rc_{SD} of each UAV is limited to one hop within its immediate
 59 neighborhood, beyond which, the UAV has to communicate via an intermediate UAV in a multi-hop
 60 manner.

61 **Assumption 3.** *In a k UAV system, the UAVs never search the same grid twice, nor do other UAVs*
 62 *sense the grid locations already covered by a UAV such that $\bigcap_k \left\{ \bigcap_{i=1}^{n^2} \mathcal{L}_i \right\} = \emptyset, \quad \forall 0 < k \leq n^2$*

63 **Assumption 4.** *Each UAV in the network is assumed to have two wireless access points – one for*
 64 *receiving the data and the other for sending the data. Once the image is processed in the assigned*
 65 *UAV, it returns the coordinates of the detected object to the central UAV of the swarm.*

66 **Definition 1.** *We consider the swarm of Edge UAVs in this work to be heterogeneous due to the*
 67 *presence of a unique sensor type on each UAV. Additionally, the sensors can be scalar, as well as*
 68 *multimedia ones.*

69 1.1. Heterogeneous Collaborative Sensing

70 We consider a $n \times n$ observation area consisting of equally divided grids. If a single UAV-based
 71 visual coverage/observation/remote sensing of an area takes x units of time in a single grid, the
 72 time taken to cover the whole observation area by a UAV becomes n^2x units of time, which results
 73 in worst-case time complexity of $T(n) = O(n^2)$. In contrast, having as many UAVs as the number
 74 of search grids incurs a time complexity of $O(1)$. However, this approach is infeasible for large
 75 deployments. Along similar lines, the use of UAVs fitted with scalar sensors for remote sensing tasks
 76 ushers in worst-case time complexity of $T(n) \simeq O(n^3)$ as it needs to sense in a 3-dimensional space
 77 due to the insufficient sensing range of these sensors. Despite the low data volume generated from
 78 these sensors, the search time of this approach is infeasible for use in time-critical tasks, except in
 79 vast numbers, which again makes the proposed approach infeasible.

80 We, therefore, propose the use of a heterogeneous swarm of UAVs for accomplishing the search
 81 task in a relatively time-efficient manner by making use of the benefits of both UAV-based multi-
 82 media, as well as scalar sensing. We attribute the heterogeneous nature of each Edge swarm to the
 83 presence of different sensors on each swarm member – either multimedia or scalar. Each of these

84 individual members of the swarm performs individual sensing tasks to achieve the more massive
 85 collective task of a time-efficient observation of an area or in a collaborative manner. Additionally,
 86 the use of multiple UAVs in farmland sensing provides resilience against individual UAV failures.
 87 However, this heterogeneity creates some unique issues such as the problem of the ratio of UAVs
 88 with multimedia sensors and UAVs with scalar sensors. Additionally, this heterogeneity also results
 89 in the problem of unequal data-rate and data-volume from each swarm member, resulting in various
 90 degrees of processing under-utilization and over-utilization within the Edge swarm. Considering Δ_l
 91 is the data generated from the UAV camera per second for a frame rate of f_{acc} , and a frame size of
 92 δ_l , the data load per second from this UAV can be expressed as $\Delta_l = \delta_l \times f_{acc}$. We summarize the
 93 whole problem as processing Δ_l in the least time possible within the UAV swarm.

94 1.2. Distributed Collaborative Processing

95 To address our problem statement, we propose an intra-swarm distributed processing scheme for
 96 mitigating the processing load from the multimedia Edge UAV node. The UAV with camera sensors
 97 offloads the majority of its processing onto other swarm members, which as per our implementation
 98 scenario, have a relatively lesser processing load on them due to the integration of scalar sensors
 99 only. Previously, the distributed processing of computationally intensive tasks has been performed
 100 with multicore parallelism and coprocessing on GPUs [7], and division of datasets for simultaneous
 101 processing on multicore processor architectures [8] with very promising reports of computation speed-
 102 ups and energy conservation. However, these approaches do not consider a highly mobile and
 103 resource-constrained environment such as the one in our case, in which processing and even data-
 104 offloading become significant factors in deciding the offload targets.

In this work, we distribute the captured video frames to other swarm members for processing. Each of these swarm members has similar processor specifications. As the member UAVs do not have a camera sensor to process their data, each of the member UAVs processes the data offloaded to them for processing, besides their regular and comparatively low-scale processing and scalar sensing tasks. If t_{UAV} is the amount of time required to process Δ_l , then for a k UAV swarm,

$$t_{UAV} = \frac{\Delta_l}{k} + \sum_{i=1}^k C_i + \sum_{i=1}^{k-1} \tau_i \quad (1)$$

105 In equation 1, C_i is a constant representing the internal processing time of the i^{th} UAV, and τ_i
 106 is the delay incurred during the transfer of one frame from one UAV to another in a single hop.
 107 To maximize processing throughput from each UAV processor by minimizing $\sum_{i=1}^k C_i$ we estimate
 108 the average processing wait times for the images at each UAV node from their respective queue
 109 properties.

110 Additionally, based on the distribution of the traffic flow in the deployed network, and the
 111 resources available at each UAV node, we formulate a joint utility function for the UAV nodes in the
 112 swarm. A Nash bargaining solution is applied to the utility function to strategize the distribution
 113 of acquired video frames from the multimedia UAV with the camera to the other UAV nodes in
 114 the swarm before deployment. This approach allows the setting of an optimum frame rate of video
 115 capture, the swarm size, and even the communication architecture of the swarm. Finally, we compare
 116 the results obtained to various star and mesh topologies. Our approach shows positive results
 117 regarding processing speed-ups, as well as scalability of deployment.

118 1.3. Contributions

119 In this work, we establish a viable means of time-critical remote sensing of ground plots and
 120 crops in smart farming. We propose the use of heterogeneous Edge UAVs in a swarm formation

121 to remotely sense a given zone – some using camera sensors, while the others using scalar sensors.
122 The unequal data-load generated and subsequently the processing load on the UAVs in the swarm,
123 due to the heterogeneous nature of this swarm, is mitigated by a Nash bargaining game to achieve
124 significant processing speed-ups and enhance the scalability of the system. The main contributions
125 of this work are:

- 126 1. A proposition for the use of heterogeneous UAV swarm consisting of mixed UAVs armed with
127 either scalar or multimedia sensors, jointly performing remote sensing over farmlands, is put
128 forward.
- 129 2. A distributed multimedia data processing approach for mitigating the processing load of a few
130 swarm members to the whole swarm is proposed to contain the processing within the Edge
131 itself.
- 132 3. A Nash bargaining based game is proposed to decide the intra-swarm offload architecture such
133 that for a given number of UAVs, the optimized offload architecture formed aims to minimize
134 processing lag, reduce the offload delay times, and allocates maximum processing resources to
135 the multimedia data offloaded.
- 136 4. An evaluation hardware consisting of four UAVs in a swarm is setup. The communication,
137 time, and energy metrics measured from the hardware is used for emulating the behavior of
138 our proposed approach for a large Edge swarm.

139 2. Related Works

140 The use of UAVs and UAV swarms has been explored for a multitude of tasks such as tracking
141 [9], path planning, and other communication aspects within [10], and outside the swarm [11]. Con-
142 cerning the objectives being pursued in this work, we divide the related works into three groups – 1)
143 Heterogeneous Collaborative Sensing, 2) UAV swarms in sensing and tracking, and 3) Distributed
144 processing in highly mobile environments.

145 2.1. Heterogeneous Collaborative Sensing

146 Heterogeneous collaborative sensing, although challenging, has been used for achieving resource-
147 efficient results as compared to traditional approaches. Typically, collaborative sensing has been
148 used for spectrum sensing and robotic swarms. Collaborative spectrum sensing has been used for
149 tasks such as radio resource allocation [12], estimating the global spectrum states [13], and others.
150 Further, approaches such as *EasiSee* [14], which is a WSN-based real-time vehicle identification
151 system, report achieving a reduction in overall energy consumption through collaborative sensing
152 using heterogeneous sensors. Collaborative sensing, especially using heterogeneous sensors, are also
153 commonly encountered in the domain of robotics and multi-robot sensor networks. Platforms such as
154 SENORA [15] and other middlewares [16] enable peer-to-peer networking and collaboration amongst
155 mobile robotic entities.

156 2.2. UAV Swarms in Sensing and Tracking

157 Works on UAV swarm-based tracking of targets on the ground, especially moving targets, present
158 solution approaches to a very challenging problem of target localization, which has huge implications
159 in real-life scenarios such as farming, surveillance, and disaster management. UAV swarm-based
160 searching involves cooperative search and tracking for targets, which may be RF-based sources [9],
161 vehicles, or even humans. These tasks involve precision in path planning and flawless coordination
162 amongst swarm members. Works by Nigam *et al.* [17] and Pitre *et al.* [18] successfully address some
163 of the challenges related to control and path planning for search and track missions respectively.

164 Nigam *et al.* [17] propose high-level aircraft control strategies, control policies for compensating
165 dynamic aircraft constraints, and health-and-endurance monitoring policies for control of multiple
166 UAVs during persistent surveillance. In contrast, Pitre *et al.* [18] take an information value approach
167 for path planning in UAV-based joint search and track missions. Their work relies on a modified
168 particle swarm optimization approach for optimizing the trajectory of the UAV to maximize the
169 targets searched. Additional tasks directly associated with multiple UAV-based searching involves
170 increasing spatial coverage distribution of sensing [19] as well as addressing connectivity management
171 issues in UAV networks [11].

172 *2.3. Distributed Processing in Highly Mobile Environments*

173 Processing offloading from low-power devices to more powerful ones is one of the widely ad-
174 dressed topics in the domain of distributed computing and processing. However, specific persistent
175 issues arise while addressing the task of processing offloading [20] in mobile environments such as
176 scalability [21] [22], bandwidth management [23], and resource allocation. Various approaches ad-
177 dressing scalability issues of distributed processing in mobile environments include those by Gedik
178 and Liu [21], where they propose a distributed architecture in conjunction with their optimization
179 techniques to address scalable processing challenges of continuously moving location queries. Their
180 approach reports significant server load and messaging cost savings in comparison to traditional
181 central processing approaches.

182 Similarly, Wu *et al.* [22] propose the use of ADDSEN, a middleware developed by them for
183 urban sensing using adaptive data processing and dissemination in UAV swarms. An online learning
184 approach periodically adjusts the broadcast rate and knowledge loss rate, whereas a strategy function
185 guides the state transitions of link status changes. Other approaches addressing various challenges
186 in distributed processing for highly mobile environments include the use of Markov chain-based
187 pattern prediction, and subsequent passive bandwidth management in QoS optimization for vehicular
188 networks, and maximizing Markovian network utility functions of multi-server systems and networks
189 in which each user may be granted resources by different servers [24].

190 *2.4. Synthesis*

191 Various works in the realm of UAV-based aerial sensing tasks rely mainly on homogenous sensing
192 platforms, which either incur massive delays in sensing (e.g., scalar sensors) or massive delays due to
193 processing (e.g., multimedia sensors) even when they are used in swarms. Typically, heterogeneous
194 and collaborative sensing rely on a central controller or server for coordinating the sensing and col-
195 laboration. A huge majority of these approaches do not consider the network or real-time processing
196 requirements of the collaborating members. Additionally, the offload of processing requirements to
197 other members in a swarm of more powerful processors is also biased regarding network bandwidth
198 considerations. A considerable majority of the works related to processing offloading do not even
199 consider the resource-constrained nature of the network or the swarm itself, where it may not always
200 be possible to offload data to remote locations over high-speed networks or have multiple high-speed
201 mobile processors. Our proposed approach of a heterogeneous collaborative Edge UAV swarm-based
202 tasks, aimed mainly at smart farming, makes use of the benefits of both scalar and multimedia
203 sensing. Our approach speeds up the time taken to sense large swathes of farmlands, and the Nash
204 bargaining based distributed processing within the swarm takes care of the high data and processing
205 load generated due to the multimedia sensors in the swarm.

206 **3. System Architecture**

A one-hop UAV data-offload architecture consists of a central UAV to which m UAVs can connect.
The UAVs can communicate with each other in a star or mesh configuration for achieving distributed

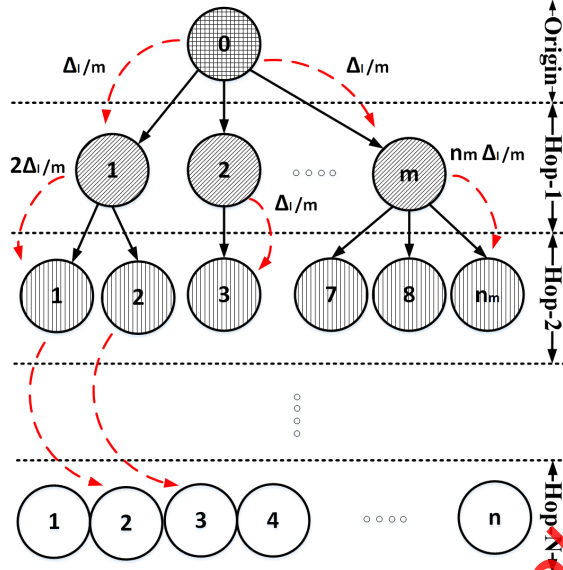


Figure 2: A representation of the multi-hop offload connection.

aerial swarm-based processing. As the connection between the UAVs is established wirelessly, each UAV connected to a central node puts a certain amount of strain on its resources. This connection-based strain on the UAV's resources is attributed to the resources consumed for maintaining the radio connection. If R_a is considered to be the total available resources at the central UAV node (node-0), then initially at $t_0|_{t=0}$ when no UAVs are connected to the central UAV node, we have $t_0 \propto R_a^{-1} \Rightarrow t_0 = \frac{K}{R_a}$ such that K is the constant of proportionality. For a k UAV system, let each UAV connection to the central UAV put a constraint on the central UAV node's resources by a factor of γ_k such that over a period, the resources consumed at the central UAV node R_c is denoted as $R_c = \gamma_1 + \gamma_2 + \dots + \gamma_{k-1} = \sum_{i=1}^{k-1} \gamma_i$. Similarly, at $t_k|_{t>0}$, for $k-1$ UAVs connected to a central UAV node, we represent t_k as:

$$t_k = \frac{R_a}{R_a - R_c} t_0 \quad (2)$$

Assumption 5. The $m-1$ UAVs connecting to a central UAV node in a m UAV system puts identical constraints on the central node's resources such that $\gamma_1 = \gamma_2 = \dots = \gamma_{m-1} = \sum_k \gamma$.

In a one-hop star connected network, n nodes connect to a central node, each contributing a lag Δ/n to the overall lag Δ of the system. The only difference between the star and mesh connected networks during distributed data processing offload is that in a star connection only the central UAV exhausts its resources with an increasing number of connections to it over a period, while in a mesh connection all nodes run out of resources at a point of time. In continuation, each UAV in a hop in a multihop UAV network approach may be connected to a few other UAVs in the next hop, however within a unit-hop distance of each other, as shown in Fig. 2. It is pertinent to mention that Fig. 2 is architecturally similar to the concept of distributed processing denoted in Fig. 1(a). Similar to the one-hop network architecture, every connection to a UAV in the multihop configuration induces a lag in that UAV's processing resources as a result of the operations required to maintain the wireless connection to the connecting UAV.

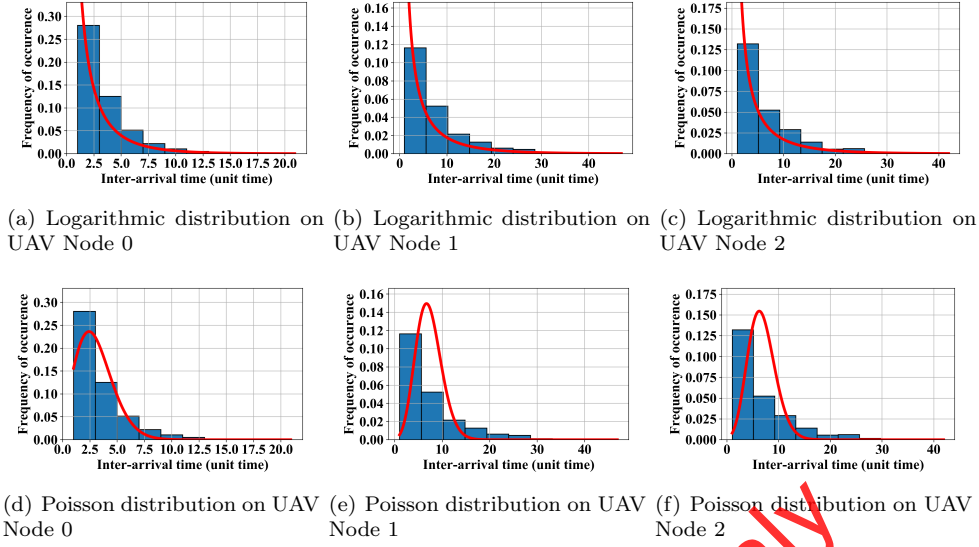


Figure 3: Fitting Poisson and Logarithmic distributions to inter-arrival times at various UAV nodes in the network and their corresponding Chi-squared parameter.

220 4. UAV Swarm Network Traffic Analysis

A multi-hop network architecture with randomized connections between the UAVs in the network is simulated, which is subject to the constraint of one-hop communication between the immediately communicating nodes. Video frames captured from the origin UAV node are allotted for processing to each immediately one-hop neighboring UAV based on the number of UAVs it is one-hop connected to and the number of the video frames already waiting to be processed by that UAV. The inter-arrival time IA for video frames arriving at every UAV in this network is calculated. The data traffic being discrete and multi-valued (not binary) is fit using Poisson and Logarithmic distributions to estimate the nature of the traffic in this network. For an event rate of λ in a network following Poisson distribution, the probability mass function (PMF) is given by:

$$f(\lambda, x) = \frac{\lambda^x e^{-\lambda}}{x!} \Big|_{x=0,1,2,\dots} \quad \forall \lambda > 0 \quad (3)$$

Similarly, the PMF of a logarithmic distribution is evaluated as:

$$f(p, x) = \frac{-1}{\ln(1-p)} \left(\frac{p^x}{x}\right) \Big|_{x \geq 1} \quad \forall 0 < p < 1 \quad (4)$$

Fig. 3 shows the result of fitting Logarithmic and Poisson distributions on the IA at various UAV nodes. Three goodness of fit (GoF) metrics – Chi-squared GoF, Akaike Information Criteria (AIC), and Pearson correlation coefficient – are calculated to determine the most appropriate distribution for the traffic in our network. The IA data is divided into x bins to calculate the Chi-square GoF, and is represented as:

$$\chi^2 = \sum_{i=1}^x \frac{(O_i - E_i)^2}{E_i}, \quad (5)$$

where, O_i is the observed frequency in the bin, and E_i is the expected frequency of IA in the bin. Again, the likelihood \mathcal{L} , which denotes the probability of the data given a model, and F free

parameters in the distribution, the AIC is calculated as,

$$\text{AIC} = -2(\log(\mathcal{L})) + 2F \quad (6)$$

Finally, for N number of IA samples with expected value x , observed value y , and mean of x and y denoted by \bar{x} and \bar{y} , respectively, the Pearson correlation coefficient is represented as:

$$\text{pearson} = \frac{\sum_{i=1}^N (x_i - \bar{x})(y_i - \bar{y})}{\sqrt{\sum_{i=1}^N (x_i - \bar{x})^2} \sqrt{\sum_{i=1}^N (y_i - \bar{y})^2}} \quad (7)$$

From the above metrics, calculated on the inter-arrival times at every node, and the corresponding results tabulated in Table 1, it is inferred that the inter-arrival times at each node in the proposed multi-hop UAV network follows a Logarithmic distribution.

Definition 2. Effective UAV Bandwidth: For m UAVs, each occupying a bandwidth of b , which is connected to a UAV with a total bandwidth of B , then $\sum_{i=1}^m b_i = mb \leq B$ and $m \leq B/b$. We term B as the Effective UAV Bandwidth, which is responsible for limiting the number of UAVs connecting to a single UAV.

Definition 3. Swarm Node Depth: It is the maximum depth (i.e., the maximum number of hops to be undertaken by an image frame) before processing. The depth of the node is limited by the Swarm Node Depth D_M such that $d \leq D_M$.

Definition 4. Inter Arrival Time: It is the time elapsed between the reception of two consecutive image frames by a UAV node. For time taken to transfer the i^{th} image frame $f(i)$ between UAVs denoted by $t_{f(i)}$, the Inter Arrival time is denoted as $IA = t_{f(i)} - t_{f(i-1)}$, $\forall i > 1$. Additionally, with respect to equation 1, it can be stated that $IA \simeq \tau$.

Definition 5. Service Time: It is the time for which the i^{th} image frame $f(i)$ resides in a UAV node, and is denoted by ST . With respect to equation 1 it can be inferred that $ST\{f(i)\} \propto C_i$.

Node	Chi-square		AIC		Pearson-coefficient	
	Poisson	Log	Poisson	Log	Poisson	Log
0	0.016	0.018	20.402	20.404	0.925	0.996
1	0.006	0.001	20.388	20.381	0.737	0.994
2	0.004	0.002	20.385	20.381	0.856	0.982
3	0.009	0.001	20.391	20.380	0.547	0.962
4	0.005	0.002	20.387	20.382	0.810	0.997

Table 1: Node wise Chi-squared GoF, Pearson correlation coefficient and AIC values for Poisson and Logarithmic distribution on IA of the network.

5. UAV Node Traffic Modeling

The IA , in our architecture, follows a Logarithmic distribution. We calculate the average waiting list of image frames at every UAV node using Queuing theory. We group the various UAV nodes in our architecture into three categories – 1) central node, 2) leaf node, and 3) intermediate node.

241 The central UAV node does not process any frames and is responsible only for video capture and
 242 frame generation, which is subsequently offloaded for processing to its immediate one-hop neighbors.
 243 Each swarm has a single central UAV node. In contrast, a UAV in the swarm with no further UAVs
 244 to offload their data to (i.e., no further children nodes present) is considered a leaf node. A leaf
 245 UAV node has to process whatever image frames get offloaded to it. Finally, any other UAV node
 246 in the network besides the central and leaf UAV nodes has two options – either process the frame
 247 by itself or assign the frame to one of its children. The data offload to other UAVs is decided from
 248 a Nash bargaining strategy-based pre-allocation of weights according to the swarm communication
 249 architecture.

In our work, we consider that the central UAV node is responsible for video capture in a swarm, whereas the other swarm members are responsible for sensing using only scalar sensors. This arrangement implies that the central UAV node is responsible for highly processing-intensive tasks, whereas the other member UAVs in the swarm have under-utilized processing resources. In our proposed multi-hop data offload scheme, considering that the tasks performed by all the UAV nodes, except the central UAV node, are not processing-intensive, the average service time ST for the processing of image frames for a fixed frame size is constant. A node's ST is only affected by the number of wireless connections to other UAV nodes maintained by it. An increase in the number of connections to a UAV node results in increased resource consumption at that node, which slows down the processing of that node leading to an increase in the time taken to process an image frame. Considering ϱ to be the percentage increase in ST for every wireless connection the UAV node is maintaining such that $\varrho \propto \gamma$, the expected ST of the node with m connections to it is formulated as:

$$E[ST] = ST_o(1 + \varrho)^m \quad (8)$$

As each connection to a UAV node increases, it slows down the concerned UAV's processing by γ , increasing the original service time of that ST_o by $1 + \varrho$. For m connections to a UAV, ST_o increases by $(1 + \varrho)^m$. We denote the mean IA rate and the mean ST by β_a and β_s , respectively. β_a and β_s can be represented as $\beta_a = E[IA]^{-1}$, $\beta_s = E[ST]^{-1}$ such that $E[.]$ represents the expectation of a random variable. The data offload mechanism in our proposed approach is similar to a $G/G/m$ queue such that the queue has m servers (UAV nodes) in which both service and the inter-arrival time have any given distribution. The IA , in our case, is distributed logarithmically (as established in Section 4), whereas the ST follows a polynomial distribution (from equation 8). For a single image frame f_i and a single processing UAV node, we formulate the utility of the UAV node as $U_s = \beta_a \beta_s^{-1}$. Along the same lines, for f_i with the choice of selecting any processing node from m UAV processing nodes, the utility of each UAV node is formulated as $U_s = \beta_a (m \beta_s)^{-1}$. Subsequently, the U_s is normalized to the maximum U_s of the system. For the sake of simplicity in calculations, we start the queue analysis of a $M/M/m$ queue, and eventually approximate it to a $G/G/m$ queue [25] when required. A $M/M/m$ queue is one in which there are m UAV nodes, and both the inter-arrival time and service time are exponentially distributed. The balance equations for a $M/M/m$ queue are formulated as:

$$\beta_a P(f_i - 1) = \begin{cases} f_i \beta_s P(f_i), & f_i \leq m \\ m \beta_s P(f_i), & \text{otherwise} \end{cases} \quad (9)$$

Using equation 9, the probability that there are f_i frames in a queue is calculated as:

$$P(f_i) = \begin{cases} P(0) \frac{(m U_s)^{f_i}}{f_i!}, & f_i \leq m \\ P(0) \frac{m^m U_s^{f_i}}{m!}, & \text{otherwise} \end{cases}, U_s \leq 1 \quad (10)$$

From equation 10 and the fact that $\sum_{f_i=0}^{\infty} P(f_i) = 1$, we calculate the probability of zero frames in

a node's queue $P(0)$ as:

$$P(0) = \left[\sum_{f_i=0}^{m-1} \frac{(mU_s)^{f_i}}{f_i!} + \frac{(mU_s)^m}{m!(1-U_s)} \right]^{-1} \quad (11)$$

Subsequently, the average number of frames in the queue of a $M/M/m$ UAV node is calculated as:

$$N_Q = \sum_{f_i=0}^{\infty} f_i P(f_i + m) = P_Q \left(\frac{U_s}{1-U_s} \right), \text{ s.t. } P_Q = \sum_{f_i=m}^{\infty} P(f_i) \quad (12)$$

From Little's theorem [26], the average waiting time W_M of a frame in a given UAV node for a $M/M/m$ queue is calculated as $W_M = \frac{N_Q}{\beta_a}$. The waiting time W_G of a frame for a $G/G/m$ queue at a UAV node can be approximated [27] as:

$$W_G \simeq W_M \left(\frac{c_a^2 + c_s^2}{2} \right) \quad (13)$$

where, c_a and c_s represent the coefficient of variation of IA and ST , respectively, and are calculated as $c_a = \sqrt{\text{variance}(IA)\beta_a^{-2}}$ and $c_s = \sqrt{\text{variance}(ST)\beta_s^{-2}}$. Similarly, the total time spent by a frame in a UAV node T_M for a $M/M/m$ queue is calculated as the sum of waiting time W_M and processing (servicing) time β_s^{-1} , and is represented as:

$$T_M = W_M + \frac{1}{\beta_s} = \frac{N_Q}{\beta_a} + \frac{1}{\beta_s} \quad (14)$$

whereas, for a $G/G/m$ queue, the total time spent by a frame in a UAV node T_G is formulated with respect to the relation in equation 13 as:

$$T_G = \left(\left(\frac{c_a^2 + c_s^2}{2} \right) W_M \right) + \frac{1}{\beta_s} \quad (15)$$

Further, applying Little's theorem, the average number of frames N at a UAV node is given by $N = \beta_a T$, which for a $M/M/m$ queue is calculated by incorporating equation 14 as:

$$N = \frac{\beta_a}{\beta_s} + N_Q \quad (16)$$

In case of our implementation, as we have previously established our system to be a $G/G/m$ one, equation 16 is rewritten by replacing N_Q with L_Q , which is the average number of image frames in the queue of a $G/G/m$ UAV node, and is approximated by Kingman [25] as:

$$L_Q = \frac{P_{Q0} U_s}{m!(1-U_s)^2} \frac{\beta_a}{\beta_s} \quad (17)$$

such that

$$P_{Q0} = \left(\sum_{k=0}^{m-1} \frac{(mU_s)^k}{k!} + \frac{(mU_s)^k}{k!(1-U_s)} \right)^{-1} \quad (18)$$

250 Equation 17 is used for calculating the queue at every UAV node in the UAV swarm network.

251 **6. Strategizing a Nash Bargaining Game**

Two cases which are encountered during processing offload from a UAV to its 1-hop neighbors are – 1) the offloading UAV node has more than one neighbor/child node and are mainly found in the intermediate levels of the offload architecture, and 2) the offloading UAV node has a single child node, which is a leaf node. Considering the case of an intermediate node, the queue at any node i is denoted by q_i . The 0^{th} node has the choice to either process the image frames itself or distribute it among its m children. The reduction of processor load at the 0^{th} node is made by distributing the processing of individual frames amongst the $m + 1$ UAV nodes such that the node and its children share the frame-wise processing to mitigate the load on the 0^{th} node itself. We assign a penalty Q_i to a UAV node for offloading its processing to other UAV nodes. The penalty for assigning a frame to a child node is taken to be the frame transfer time t_{ld} between these nodes, whereas the penalty of processing the frame within the UAV node is t_{lc} , which is attributed to the increase in processing time of the node as a result of the connections maintained by the 0^{th} node. Another metric – strength of a node S_i – is considered for use in the penalty function Q_i such that for a UAV node i , its corresponding s_i denotes the number of child nodes under it such that $1 < s_i \leq m$. To embed these penalties Q_i is defined such that,

$$Q_i = \begin{cases} (q_i s_i)/t_{lc}, & i = 0 \\ (q_i s_i)/t_{ld}, & \text{otherwise} \end{cases} \quad (19)$$

The minimum probability with which a frame is assigned to a UAV node for processing is formulated as:

$$P_{min}^i = \frac{Q_i}{\sum_{j=0}^m Q_j} \quad (20)$$

Additionally, another parameter – rank R_i – is assigned to P_{min}^i for each UAV node. R_i for the i^{th} UAV node is formulated based on its depth d_i in the network with respect to the total depth of the network D_i , and is represented as $R_i = 1/(D_i - d_i)$ such that $D_i \geq 1$ and $d_i \geq (D_i - 1)$. Subsequently, the minimum probability of assigning a frame to the i^{th} UAV node for processing with respect to equation 20 and R_i is reformulated as:

$$P_{min}^i = \frac{Q_i R_i}{\sum_{j=0}^m Q_j} \quad \forall 0 \leq i \leq m \quad (21)$$

The utility of the i^{th} UAV node for processing offloading is formulated in terms of P_{min}^i , the probability of assigning an image frame to node i denoted by P_i , and child nodes under the i^{th} UAV node denoted by c_i is given by:

$$U_i(P_i) = \frac{P_i - P_{min}^i}{c_i + 1} \quad (22)$$

P_i for each UAV node, for a given UAV swarm architecture, is calculated prior to operation of the swarm using Nash bargaining (discussed later in this section), subject to the constraints $P_i \geq P_{min}^i$ and $\sum_{i=0}^m P_i = 1$. A set S denoting the joint utility function of all UAV nodes in the swarm is defined for this work such that

$$S = \{U_0(P_0), U_1(P_1), U_2(P_2), \dots, U_m(P_m)\} \quad (23)$$

Equation 22 with respect to its constraints can be rewritten and represented for all the UAV nodes in the swarm as:

$$\begin{aligned} \sum_{i=0}^m P_i &= \sum_{i=0}^m P_{min}^i + \sum_{i=0}^m U_i(P_i)(c_i + 1) = 1 \\ \Rightarrow \sum_{i=0}^m U_i(P_i)(c_i + 1) &\leq 1 - \sum_{i=0}^m P_{min}^i \end{aligned} \quad (24)$$

From equations 23 and 24, the joint utility function S of the UAV swarm is generalized to

$$S = \left\{ U_i(P_i) \mid \sum_{i=0}^m U_i(P_i)(c_i + 1) \leq 1 - \sum_{i=0}^m P_{min}^i \right\} \quad (25)$$

252 To establish the existence of the formulated utility function $U_i(P_i)$, the joint utility function S of
253 the UAV nodes within the domain of the network proposed $i \in [0, m]$ has to be convex.

254 **Theorem 1.** *The joint utility function S of all the UAV nodes in the swarm is convex such that*
255 *$f : U_i(P_i) \mid \sum_{i=0}^m U_i(P_i)(c_i + 1) \leq 1 - \sum_{i=0}^m P_{min}^i, \forall 0 \leq i \leq m$.*

For a function $F : (P, P_{min}) \rightarrow \mathbb{R}^{+(m+1)} \forall 0 \leq m$ representing the solution for the weight allocation to the UAV nodes using the proposed Nash bargaining strategy, we consider the case of only one child UAV node connected to an offloading UAV. The optimization function is formulated as $F(P, P_{min}) = \arg \max_{P_1, P_2} U_1(P_1)U_2(P_2)$, which is rewritten as –

$$F(P, P_{min}) = \arg \max_{P_1, P_2} \frac{(P_1 - P_{min}^1)(P_2 - P_{min}^2)}{(c_1 + 1)(c_2 + 1)} \quad (26)$$

256 A Nash bargaining strategy can hold iff $F(P, P_{min})$ satisfies the criteria of Pareto efficiency, sym-
257 metry, invariance to linear transformation, and is independent of irrelevant alternatives. These
258 four conditions validate the consideration of a utility function in a bargaining problem such that it
259 provides a proportionally fair solution.

260 **Lemma 1.** *The proposed solution for the allocation of weights to the UAV nodes $F(P, P_{min})$ is*
261 *Pareto-optimal, symmetric, invariant to linear transform, and independent of irrelevant alternatives.*

Theorem 2. *There exists a unique solution for the weight allocation among the UAV nodes, which satisfy the four Nash axioms, and this solution to the optimization problem is the pair $(P_1, P_2) \in P$ such that $(P_1, P_2) \geq (P_{min}^1, P_{min}^2)$ that solves $F(P, P_{min}) = \arg \max_{P_1, P_2} U_1(P_1)U_2(P_2)$, which can also be rewritten as:*

$$F(P, P_{min}) = \arg \max_{P_1, P_2} \frac{(P_1 - P_{min}^1)(P_2 - P_{min}^2)}{(c_1 + 1)(c_2 + 1)} \quad (27)$$

262 Here, $(P_1 - P_{min}^1)(P_2 - P_{min}^2)$ is termed as the Nash product.

263 6.1. Solution to the Nash Bargaining Problem

The optimization function, which allocates weights to the various UAV nodes for a weighted distributed processing offloading within the m UAV nodes in the aerial swarm follows the four conditions or Nash axioms. A unique solution to the optimization function $F(P_i, P_{min}^i)$ is derived

Algorithm 1 Swarm Frame Distribution Algorithm

```
1: Inputs:( $Camera_{ID}$ ,  $Camera_{fps}$ )
2: Outputs:( $Tracked_{coordinates}$ )
3: Initialize:
4: Add  $Camera_{ID}$  to  $Network$ 
5:  $Network = Discover\_nodes(Camera_{ID}, Network)$ 
6:  $Queue = cal\_queue(Network, Camera_{fps})$ 
7:  $Weights = cal\_weights(Network, Queue)$ 
8:  $flag, frame = capture(Camera_{ID})$ 
9: while  $flag$  do
10:    $Target = get\_Optimal\_node(Network, Weights)$ 
11:    $Tracked_{coordinates} = Process(frame, Target)$ 
12: end while
```

using the Lagrange Multiplier method. Now considering the weight allocation among the UAV nodes in the swarm, the optimization function subject to $\sum_{i=0}^m P_i = 1$, $P_i \geq P_{min}^i$ is $F(P, P_{min}) = \arg \max_P \prod_{i=0}^m U_i(P_i)$, and is simplified as:

$$F(P, P_{min}) = \arg \max_P \sum_{i=0}^m \log \left(\frac{P_i - P_{min}^i}{c_i + 1} \right) \quad (28)$$

We solve equation 28 using Lagrange Multiplier λ , the function of which is formulated as:

$$L = \sum_{i=0}^m \log \left(\frac{P_i - P_{min}^i}{c_i + 1} \right) - \lambda \left(\sum_{i=0}^m P_i - 1 \right) \quad (29)$$

We arrive at the solution the optimization function in equation 28 considering $\frac{\partial L}{\partial P_i} = 0$ and $\frac{\partial L}{\partial \lambda} = 0$. This also ensures that the solution maximizes the optimization problem. A total of $(m + 1) + 1$ equations are obtained, the solutions to which can be generalized to obtain the weight assigned to i^{th} node as:

$$P_i = P_{min}^i + \frac{(1 - \sum_{i=0}^m P_{min}^i)}{m + 2} \quad (30)$$

264 6.2. Weight Allocation to UAV Nodes in the Swarm

265 All the UAV nodes other than central and leaf UAV nodes have two probabilities – one with
266 which its parent UAV node assigns it a frame, and the other with which it processes the frame by
267 itself without passing it to its child node. The central UAV node does not process any image frames
268 and acts as a client in a client-server communication analogy. Post-assignment of an image frame
269 for processing, a leaf UAV node does not have the option of offloading their processing to other
270 UAV nodes and act only as servers. The intermediate nodes act as both clients as well as servers.
271 Algorithm 1 outlines the image frame distribution scheme for processing mitigation to member UAV
272 nodes in a heterogenous UAV swarm. Algorithm 1 is responsible for the distribution of the generated
273 image frames within the swarm members, depending on the network traffic and available processing.
274 Initially, given the ID of the central UAV node with the attached camera sensor, and information
275 of the camera's capture rate in frames per second (fps), a network is formed by the central UAV
276 node by polling for UAVs in its vicinity and within its swarm using Algorithm 2.

277 Algorithm 2 on a UAV node first checks whether the node is a child node or not. IF at first
 278 pass, the node does not find any parent nodes, it becomes the parent node (root node). Further, if
 279 it is a child node, it establishes a connection with the parent node upon satisfying the bandwidth
 280 requirements for data offloading. Similarly, the node checks for the presence of child nodes under it,
 281 the detection of which results in running Algorithm 2 in these child nodes. This process keeps on
 282 repeating until there are no child nodes left to discover (all the current nodes are leaf nodes).

Algorithm 2 UAV Node Discovery Algorithm

```

1: Inputs:(Node, Network)
2: Outputs:(Network)
3: Initialize (Discover_nodes):
4: child = check(Parent)
5: for each Node in child do
6:   Establish connection between Parent and node in Network if the Bandwidth constraint is
   satisfied
7:   child_child = check(Node)
8:   for each Node in child_child do
9:     Network = Discover_nodes(Node, Network)
10:  end for
11: end for

```

283 Once the network is formed, the average queue length at every UAV node is calculated using
 284 equation 16. The information of the estimated queue lengths at each UAV node enables the as-
 285 signment of weights to each of these nodes. The image frames captured at the central UAV node
 286 are assigned to available UAV nodes for processing using Algorithm 3. This algorithm first checks
 287 whether the current node is the root node and whether it has children nodes (*child_*). If the cur-
 288 rent node has only one level of children nodes (which will be leaf nodes of the generated graph), it
 289 randomly selects any one of the children nodes for acting as servers during the distributed process-
 290 ing. Otherwise, the child node can act as a data generator (consumer) as well as a data processor
 291 (server). This is repeated until the leaf nodes are reached. Algorithm 3 thus decides its target nodes.
 292 The list of these selected nodes is returned to Algorithm 1. The selected nodes process the offloaded
 293 images using a pre-trained visual tracking algorithm and return the coordinates (*Tracked_{coordinates}*)
 294 of tracked humans to the central UAV node.

295 **7. Performance Evaluation**

296 This section is divided into two parts – 1) Evaluation hardware setup and 2) Simulation. The UAV
 297 network architectures used for comparison are recreated using four real-life UAVs with externally
 298 mounted Raspberry Pi processors to obtain network metrics from these implemented UAVs, as
 299 shown in Fig. 4. Large-scale simulation of the network is performed based on the real-life network
 300 metrics obtained and tuned into our custom-made simulator developed in Python. The network
 301 traffic and performance metrics from the real-life, small-scale UAV network is used for realistically
 302 guiding the behavior of the large-scale network of UAVs formed, which holds even for different
 303 network configurations using the same radio protocol (in our case, WiFi).

304 *7.1. Evaluation Hardware Setup*

305 A pilot-scale implementation of an aerial swarm using 4 UAVs is implemented, as shown in Fig.
 306 4. Every member of the swarm is armed with unique sensors – scalar, as well as multimedia. For

Algorithm 3 Optimal Node Selection Algorithm

```
1: Inputs:(Network,Weights)
2: Outputs:(Target)
3: Initialize:
4: count = 1
5: Node = Network → root
6: while True and (Node != NULL) do
7:   child_ = Node → child
8:   if count = 1 then
9:     Target = randomly select a Node among the child_ with the probabilities of them being
     servers.
10:  else
11:    Target = randomly select a Node among the child_ and the Node itself with the proba-
    bilities of them being servers and consumer respectively.
12:  end if
13:  if Target == Node then
14:    return(Target)
15:  else
16:    Node = Target
17:  end if
18: end while
```

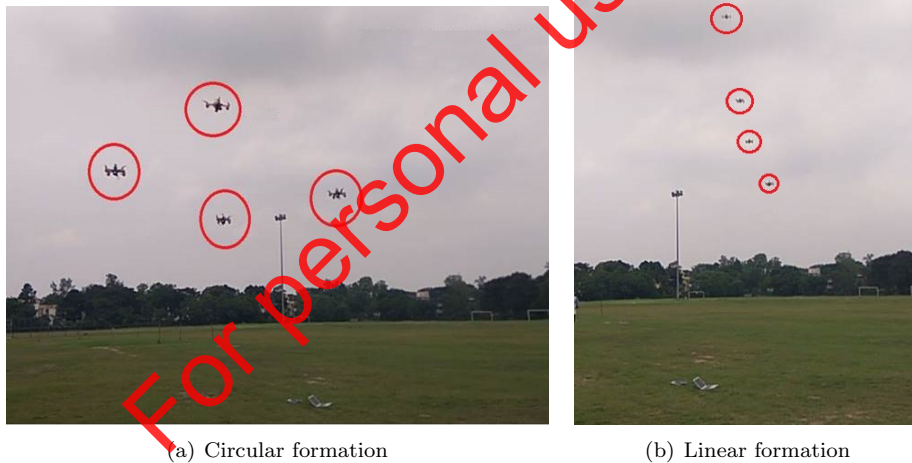


Figure 4: A pilot-scale UAV swarm implementation.

307 our work, we use a single camera-armed UAV. The other three UAVs in the network are armed with
308 just scalar sensors. Initially, we use a standard video to test a Faster RCNN-based approach [28]
309 for tracking ground targets (in our case, humans) in successive video frames. This model can be
310 easily trained for use with UAV-based aerial videos of humans on the ground. However, as a part of
311 this work addresses UAV-based visual tracking of human targets on the ground, the Faster RCNN
312 module has been implemented on the low-power processors on the UAV. This implementation results
313 in massive delays in computation and video frame-wise tracking. Additionally, the substantial power

314 requirements of GPUs acts as a deterrent for its use on the small-scale UAVs, especially quadrotors.
 315 Typically in our case, a GPU takes 0.2 seconds, a CPU server takes 7 seconds, and the processor
 316 on the UAV (a Raspberry Pi module) takes 90 seconds to process a single video frame. A single
 317 UAV tasked with executing the tracking task on its own would severely deteriorate the efficiency
 318 of the said UAV's processing system and would be too slow to be of any use in real-time tracking
 319 of humans/targets on the ground. Further, ST_0 is calculated by allowing a single UAV with no
 320 connections to implement the Transfer-learning (Faster RCNN) based visual object detection on a
 321 single video frame. Similarly, τ is estimated according to the time taken to process the single frame
 322 by the UAV with a subsequently increasing number of connections to it. Finally, the transfer time of
 323 an image frame between UAVs is calculated by transmitting and receiving an image frame between
 324 two UAVs over a Wi-Fi link between the UAVs. The actual values of ST_0 , τ , and T_f obtained from
 325 one of our UAVs in real-time are 90 seconds, 5%, and 0.005 seconds, respectively for a video frame
 326 size of $1KB$. Fig. 5 shows the results of the large-scale implementation of our proposed approach,
 327 and its comparison against the benchmark architectures for an incoming video frame rate of $25fps$
 328 from the origin UAV.

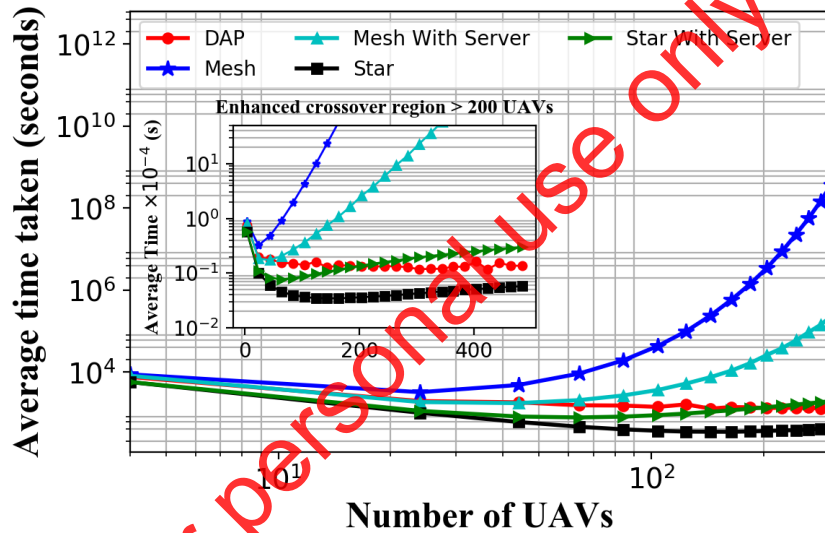


Figure 5: Comparison of the average processing time in the network taken for a frame-rate of $25fps$ among various architectures. Both x and y axes are on the log-scale. Only the y axis of the inset plot is on the log-scale.

329 7.2. Simulation

330 Simulation is performed to emulate UAV swarm networks of varying architectures, given the
 331 number of UAVs, processing time of single image frame on a UAV node with zero connections
 332 (ST_0), percentage increase in the processing time for every maintained UAV connection ($\tau \propto \gamma$), and
 333 wireless transfer time of data between two UAVs (T_f). Three broad classes of network connections are
 334 considered during our simulation – 1) the proposed multi-hop network architecture, 2) star connected
 335 network architecture, and 3) mesh connected network architecture. The simulation for the multi-hop
 336 architecture, which is the solution provided in our work, is based on Algorithm 1. This algorithm
 337 estimates the length of the queue at each UAV node from the inter-arrival times and then assigns

338 appropriate weights to those UAV nodes, which helps in uniform processing resource utilization
 339 across the whole network, without unduly burdening a select few UAV nodes. In contrast, in the
 340 architectures based on one-hop communication, e.g., a connected star network, the image frames
 341 are equally distributed among the UAVs as all of them are equidistant from the central UAV and
 342 process similar resources. Finally, in the mesh connected network architecture, the current waiting
 343 list of image frames at each UAV node is considered before assigning that UAV node with an image
 344 frame to process.

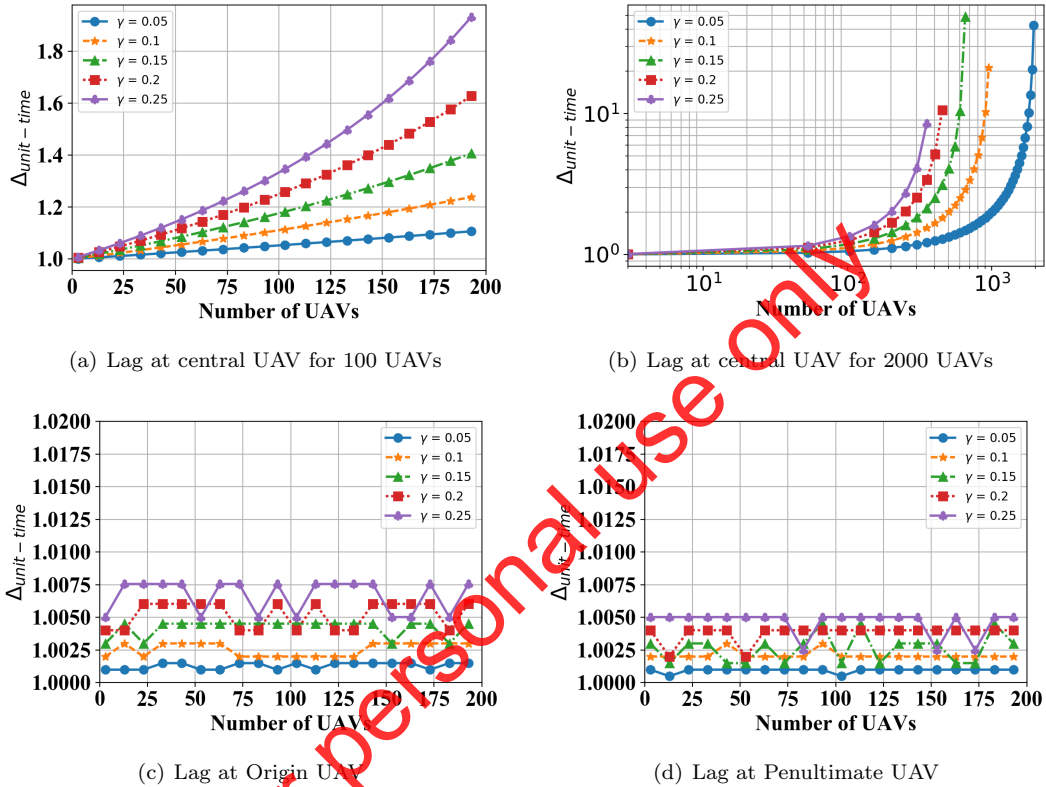


Figure 6: Calculated metrics (lag) for UAV network connection – one-hop star and DAP – architectures.

345 The performance of the proposed distributed aerial processing (DAP) is compared against the
 346 following regular UAV network architectures – 1) Star, 2) Star with a ground server, 3) Mesh, and
 347 4) Hierarchical mesh. The UAVs in a star network communicate through a central UAV, which
 348 is connected through a one-hop link only. The number of UAVs that can simultaneously connect
 349 to the central UAV is limited due to γ of the central UAV, which results in limited scalability of
 350 the network. It is similar to the architecture explored in [29] [30]. In continuation, the UAVs in a
 351 star with a ground server network communicate through a central server on the ground, which is
 352 connected to the UAVs through a one-hop link only. The number of UAVs that can simultaneously
 353 connect to the central UAV is limited due to γ of the central UAV, which results in limited scalability
 354 of the network. It is similar to the architecture explored in [31].

355 The UAVs in a mesh network can all communicate with each other employing multiple hops via
 356 intermediate UAVs and is similar to the architecture in [32]. However, during processing offloading,

357 the processing distribution on all UAVs is not symmetrical, resulting in UAVs with unequal load
 358 distribution in addition to the extra time taken to offload the data within the network nodes. Further,
 359 the hierarchical mesh network of UAVs is divided into two halves [33]. In each of the halves, all the
 360 UAVs are connected in a mesh. The communication between the meshes is through a ground server,
 361 which results in bottlenecks during processing and data offload.

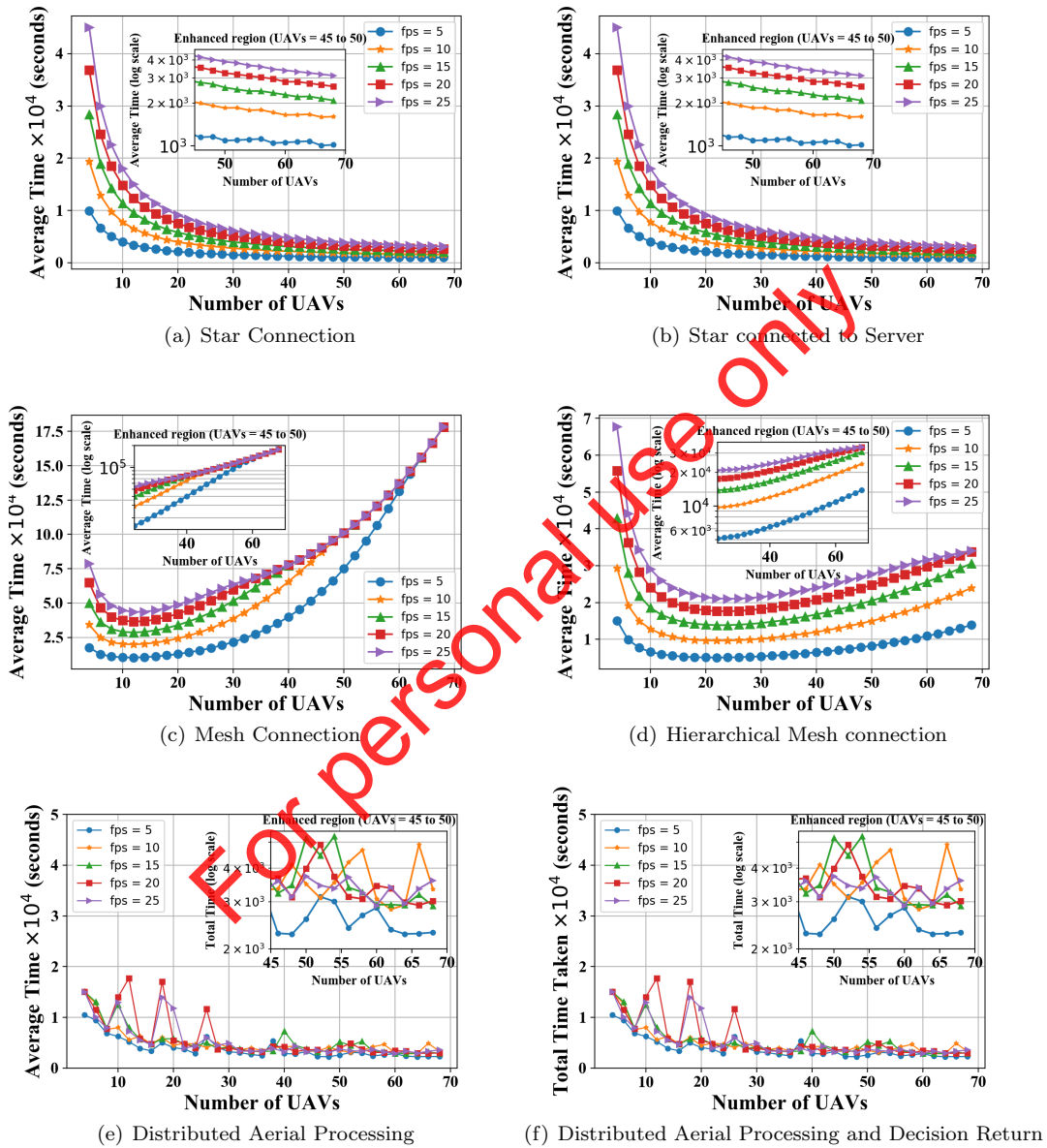


Figure 7: Comparison of the average processing time to increasing UAV swarm size and changes in the incoming video frame-rate fps for all benchmark architectures. The y axes of all the inset plots from (a) to (f) are on log-scale.

362 8. Results

363 This section is divided into four sub-sections to analyze the real-life, hardware metric tuned simu-
364 lation of large-scale UAV network topologies – 1) inter-topology performance, 2) network scalability,
365 3) inter-topology processing time performance, and 4) collective network processing speed.

366 8.1. Inter Topology Performance

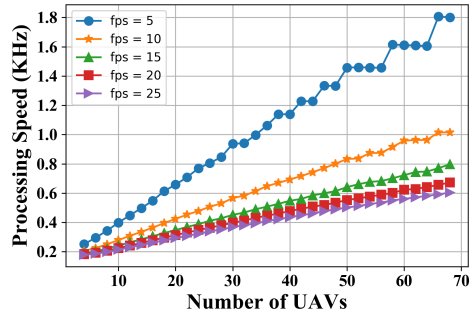
367 Fig.5 shows the average time taken to process video frames at 25 *fps* for various architectures. It is
368 seen that the overall processing time taken for the mesh and hierarchical mesh architectures increase
369 with the increase in the number of UAV nodes in the network. **The average time taken to process
370 frames gradually reduces till a saturation point for each configuration is reached. For each of these
371 saturation points, the corresponding network topology can no longer support collaborative processing
372 and offload, which manifests itself in the form of an exponential increase in the average processing
373 times.** This is attributed mostly to the transfer time incurred during data offloading between the
374 UAV nodes. **The mesh configurations are the first ones to saturate as this topology itself involves
375 data duplication between the network links to ensure network transfer reliability. In contrast, the
376 star topologies ensure better data accommodation through the network links owing to the central
377 controller.** Further, the average processing time taken for the star architectures are comparatively
378 lesser, which is attributed to the one-hop-only data offload restrictions. **It is additionally seen that
379 DAP initially behaves similar to a mesh network (performs better than mesh but poorer than star
380 topologies), but gradually, for 200 UAV nodes, DAP surpasses the performance of start topology
381 with a ground server (refer Fig. 5). As DAP maintains symmetrical distribution processing time
382 among all the UAV nodes in the network, a more balanced and enhanced performance is projected
383 for an increasing number of UAV nodes in the network.**

384 8.2. Network Scalability

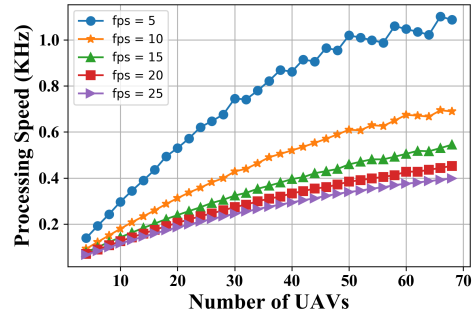
385 Fig. 6 shows the comparative performance of the star topology and our proposed DAP, regarding
386 the scalability of the architecture. In Figs. 6(a) and 6(b), it is seen that for increasing γ , and
387 increasing UAVs in the network, the data processing lag Δ increases and eventually saturates for
388 larger number of UAVs (Fig. 6(b)). In contrast, the multihop topology followed by DAP results in
389 constant lag for an increasing number of UAVs, as seen in Figs. 6(c) and 6(d). Unlike star topology,
390 the processing load in DAP is evenly distributed across the network members. It is seen in Fig. 6(c)
391 that Δ at the root or origin node is comparable to the one at the intermediate nodes (as shown in
392 Fig. 6(d)). Summarizing the scalability, we see that star configuration has limited scalability and
393 saturates beyond a point which manifests itself in the form of an unrealistic increase in processing
394 time (as shown in Fig. 6(b)). In contrast, the proposed DAP approach takes a balanced approach
395 of uniform scalability and proportional distribution processing time among all the UAV nodes in the
396 network.

397 8.3. Inter Topology Processing Times

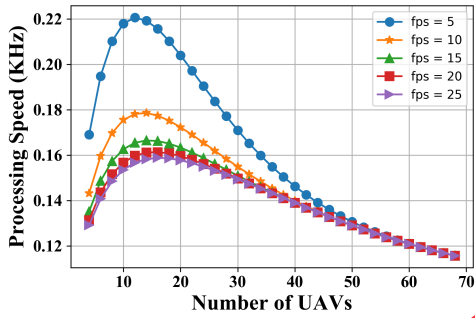
398 Fig. 7 shows the average time taken to distribute and process video frames for various architec-
399 tures with varying video frame rates (in *fps*). The star (Fig. 7(a)) and the server connected star
400 (Fig. 7(b)) networks show a drop in average processing time with an increase in the number of UAV
401 nodes. Additionally, as the frame rate of the video being offloaded increases, the processing time
402 goes up. In contrast, for the mesh (Fig. 7(c)) and hierarchical mesh (Fig. 7(d)) UAV networks, the
403 average processing time increases with an increase in the number of UAV nodes. In mesh networks,
404 it is seen that using the constraints outlined in the previous section, the average processing time for
405 all frame rates converges, which is attributed to the processing overloading of the UAV nodes in that



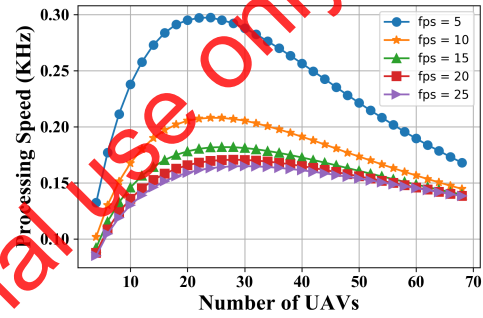
(a) Star Connection



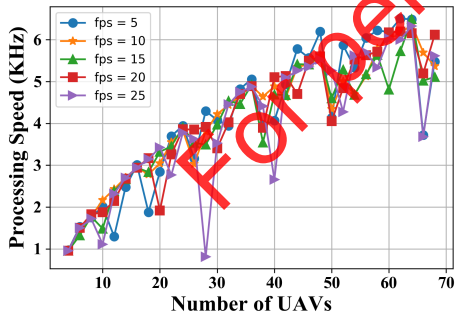
(b) Star connected to Server



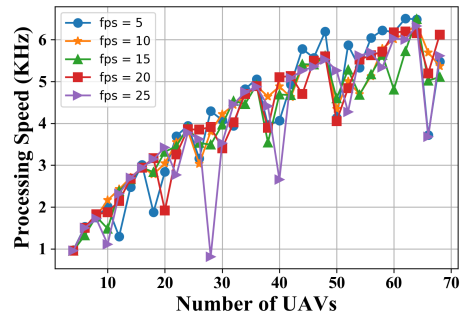
(c) Mesh Connection



(d) Hierarchical Mesh connection



(e) Distributed Aerial Processing



(f) Distributed Aerial Processing and Decision Return

Figure 8: Comparison of the average collective network processing speed available with respect to increasing UAV swarm size and changes in the incoming video frame-rate fps for all benchmark architectures. The y axes of all the inset plots from (a) to (f) are on log-scale.

406 network. For hierarchical mesh, this convergence occurs much later on. Finally, in the proposed
 407 DAP scheme in Figs. 7(e) and 7(f), the initial average processing time is much lower than that
 408 of the other configurations, and starts decreasing with an increasing number of UAV nodes. The
 409 sudden peaks obtained in the plots are attributed to the random arrangement of the UAV nodes in
 410 the architecture, wherein some nodes may not always have a child node to offload its processing.
 411 Fig. 7(f) depicts the total time taken to process the image frames and return the detected object's
 412 coordinates to the origin UAV. As the detected coordinates of the bounding box incur very low data
 413 load, this return operation takes negligible time.

414 8.4. Collective Network Processing Speed

415 Fig. 8 shows the available collective processing speed of the network in kHz. In Figs. 8(a) and
 416 8(b), it is seen that as the network size goes up, the collective processing speed of the network for
 417 various values of γ increases. However, for the available real-life hardware metrics, it is observed that
 418 for approximately 200 UAVs in the star and its associated network, the collective network processing
 419 speed reaches 3 kHz, saturates, and eventually drops to 1 kHz. This sudden drop is attributed to
 420 the exhaustion of all processing resources at the offloading central UAV of the star topology. In
 421 contrast, for the mesh and hierarchical mesh topologies (as shown in Figs. 8(c) and 8(d)), reduction
 422 in the available processing speed of the topology starts at approximately 15 UAVs for regular mesh
 423 and 20 UAVs for the hierarchical mesh. The maximum collective network speed achieved is in the
 424 range of 0.3 kHz, which is much lesser than that of the star topology. The poor performance of mesh
 425 topology is attributed to the resources spent in establishing peer connections in the network, which
 426 leaves very little for the processing of image frames. Eventually, it is seen that DAP outperforms
 427 all the topologies regarding the collective network processing speed. In Figs. 8(e) and 8(f), we see
 428 that although some UAVs show a fall in their individual available processing speeds, the collective
 429 processing speed of the network increases with increase in the number of UAVs in the network. For
 430 the available hardware metrics, DAP achieves a collective network speed of approximately 6 kHz,
 431 which is double that of star topology for a fraction of UAVs.

432 9. Conclusion

433 This work proposes an intra-UAV swarm processing offloading scheme to mitigate the problem of increased processing delays due to processing-intensive tasks such as visual identification of farmlands, crop health monitoring, and crop growth tracking. Our proposed weighted offloading is governed by the use of a Nash bargaining game between the probability of a node processing the data itself or offloading it to a child node by a queueing theory-based analysis of the network traffic in the said swarm. Real-life hardware metrics calculated from our actual 4 UAV system are used for tuning simulations of a large number of UAVs following various network topologies. The results show that unlike star networks, our proposed DAP scheme is highly scalable, and for a larger number of UAVs, performs faster than star networks, as shown in Fig. 5. DAP always outperforms the mesh topology regarding average processing times. Interestingly, our approach outperforms both the star and mesh topologies regarding collective network processing speeds available such that even for a fraction of the UAVs in star and mesh topologies, DAP achieves double the collective speeds up of a star topology. The average processing times, although very high for our tuned hardware metrics due to restrictions of the hardware used (Raspberry Pi), establishes the immense usability and benefits of our approach in comparison to other topologies.

448 In the future, we plan to study our DAP approach by incorporating resource-constrained and
 449 low-footprint visual identification and tracking algorithms.

450 **Acknowledgement**

451 This work is supported by Information Technology Research Academy (ITRA), Government of
452 India under ITRA-Water Grant ITRA/15(69)/WATER/M2M/01.

453 **References**

- 454 [1] Akyildiz IF, Kak A. The Internet of Space Things/CubeSats: A ubiquitous cyber-physical
455 system for the connected world. *Computer Networks* 2019;150:134–49.
- 456 [2] Erdelj M, Król M, Natalizio E. Wireless sensor networks and multi-UAV systems for natural
457 disaster management. *Computer Networks* 2017;124:72–86.
- 458 [3] Sun P, Boukerche A. Performance modeling and analysis of a UAV path planning and target
459 detection in a UAV-based wireless sensor network. *Computer Networks* 2018;146:217–31.
- 460 [4] Shigekuni T, Ushio T, Azumi T. Cloud-assisted sensing and supervision of multiple unmanned
461 aerial vehicles by a single operator. In: *Proceedings of the ACM/IEEE Sixth International
462 Conference on Cyber-Physical Systems. ICCPS '15; New York, NY, USA*. ACM. ISBN 978-1-
463 4503-3455-6; 2015, p. 254–.
- 464 [5] Gupta L, Jain R, Vaszkun G. Survey of important issues in uav communication networks. *IEEE
465 Communications Surveys & Tutorials* 2016;18(2):1123–52.
- 466 [6] Sharafeddine S, Islambouli R. On-demand deployment of multiple aerial base stations for traffic
467 offloading and network recovery. *Computer Networks* 2019;.
- 468 [7] Wachowiak MP, Timson MC, DuVal DJ. Adaptive Particle Swarm Optimization with Het-
469 erogeneous Multicore Parallelism and GPU Acceleration. *IEEE Transactions on Parallel and
470 Distributed Systems* 2017;28(10):2784–98.
- 471 [8] Karimipour H, Dinavahi V. Parallel Domain-Decomposition-Based Distributed State Es-
472 timation for Large-Scale Power Systems. *IEEE Transactions on Industry Applications*
473 2016;52(2):1265–9.
- 474 [9] Koohifar F, Kumbhar A, Guvenc I. Receding Horizon Multi-UAV Cooperative Tracking of
475 Moving RF Source. *IEEE Communications Letters* 2017;21(6):1433–6.
- 476 [10] Rao S, Ghose D. Sliding Mode Control-Based Autopilots for Leaderless Consensus of Unmanned
477 Aerial Vehicles. *IEEE Transactions on Control Systems Technology* 2014;22(5):1964–72.
- 478 [11] Goddemeier N, Daniel K, Wietfeld C. Role-Based Connectivity Management with Realistic Air-
479 to-Ground Channels for Cooperative UAVs. *IEEE Journal on Selected Areas in Communications*
480 2012;30(5):951–63.
- 481 [12] Sardellitti S, Barbarossa S. Joint optimization of collaborative sensing and radio resource
482 allocation in small-cell networks. *IEEE Transactions on Signal Processing* 2013;61(18):4506–20.
- 483 [13] Xu Y, Cheng P, Chen Z, Li Y, Vucetic B. Mobile Collaborative Spectrum Sensing for Het-
484 erogeneous Networks: A Bayesian Machine Learning Approach. *IEEE Transactions on Signal
485 Processing* 2018;66(21):5634–47.

- 486 [14] Wang R, Zhang L, Xiao K, Sun R, Cui L. EasiSee: Real-time vehicle classification and counting
487 via low-cost collaborative sensing. *IEEE Transactions on Intelligent Transportation Systems*
488 2013;15(1):414–24.
- 489 [15] Rahman MA, Miah MS, Gueaieb W, El Saddik A. SENORA: A P2P service-oriented framework
490 for collaborative multirobot sensor networks. *IEEE Sensors Journal* 2007;7(5):658–66.
- 491 [16] Gerasimou S, Matragkas N, Calinescu R. Towards systematic engineering of collaborative
492 heterogeneous robotic systems. In: *Proceedings of the 2nd International Workshop on Robotics
493 Software Engineering*. IEEE Press; 2019, p. 25–8.
- 494 [17] Nigam N, Bieniawski S, Kroo I, Vian J. Control of Multiple UAVs for Persistent Surveil-
495 lance: Algorithm and Flight Test Results. *IEEE Transactions on Control Systems Technology*
496 2012;20(5):1236–51.
- 497 [18] Pitre RR, Li XR, Delbalzo R. UAV Route Planning for Joint Search and Track Missions –
498 An Information-Value Approach. *IEEE Transactions on Aerospace and Electronic Systems*
499 2012;48(3):2551–65.
- 500 [19] Daniel K, Rohde S, Goddemeier N, Wietfeld C. Cognitive Agent Mobility for Aerial Sensor
501 Networks. *IEEE Sensors Journal* 2011;11(11):2671–82.
- 502 [20] Li K. A Game Theoretic Approach to Computation Offloading Strategy Optimization for Non-
503 cooperative Users in Mobile Edge Computing. *IEEE Transactions on Sustainable Computing*
504 2018;.
- 505 [21] Gedik B, Liu L. MobiEyes: A Distributed Location Monitoring Service Using Moving Location
506 Queries. *IEEE Transactions on Mobile Computing* 2006;5(10):1384–402.
- 507 [22] Wu D, Arkhipov DI, Kim M, Talcott CL, Regan AC, McCann JA, et al. Addsen: Adaptive
508 data processing and dissemination for drone swarms in urban sensing. *IEEE Transactions on
509 Computers* 2017;66(2):183–98.
- 510 [23] Fazio P, Tropea M, Rango FD, Voznak M. Pattern Prediction and Passive Bandwidth Man-
511 agement for Hand-over Optimization in QoS Cellular Networks with Vehicular Mobility. *IEEE
512 Transactions on Mobile Computing* 2016;15(11):2809–24.
- 513 [24] Teymoori P, Sohraby K, Kim K. A Fair and Efficient Resource Allocation Scheme for
514 Multi-Server Distributed Systems and Networks. *IEEE Transactions on Mobile Computing*
515 2016;15(9):2137–50.
- 516 [25] Kingman J, Atiyah M. The single server queue in heavy traffic. *Operations management:
517 critical perspectives on business and management* 2003;57:40.
- 518 [26] Little JD. A proof for the queuing formula: $L = \lambda w$. *Operations research* 1961;9(3):383–7.
- 519 [27] Bertsimas DJ, Van Ryzin G. Stochastic and dynamic vehicle routing in the Euclidean plane
520 with multiple capacitated vehicles. *Operations Research* 1993;41(1):60–76.
- 521 [28] Ren S, He K, Girshick R, Sun J. Faster R-CNN: Towards Real-Time Object Detection with
522 Region Proposal Networks. *IEEE Transactions on Pattern Analysis and Machine Intelligence*
523 2017;39(6):1137–49.

- 524 [29] Saad W, Han Z, Basar T, Debbah M, Hjorungnes A. A selfish approach to coalition formation
525 among unmanned air vehicles in wireless networks. In: 2009 International Conference on Game
526 Theory for Networks. 2009, p. 259–67.
- 527 [30] Erdelj M, Natalizio E, Chowdhury KR, Akyildiz IF. Help from the sky: Leveraging uavs for
528 disaster management. *IEEE Pervasive Computing* 2017;16(1):24–32.
- 529 [31] Sivakumar A, Phang TS, Tan CKY, Seah WKG. Robust airborne wireless backbone using
530 low-cost UAVs and commodity WiFi technology. In: 2008 8th International Conference on ITS
531 Telecommunications. 2008, p. 373–8.
- 532 [32] Sbeiti M, Goddemeier N, Behnke D, Wietfeld C. PASER: Secure and Efficient Routing Approach
533 for Airborne Mesh Networks. *IEEE Transactions on Wireless Communications* 2016;15(3):1950–
534 64.
- 535 [33] Bok PB, Tuchelmann Y. Context-aware qos control for wireless mesh networks of uavs. In:
536 2011 Proceedings of 20th International Conference on Computer Communications and Networks
537 (ICCCN). 2011, p. 1–6.

For personal use only